

Corrosion Behavior of 7075-T6 Aluminum Alloy in the Presence of *Aspergillus Niger*

Qi Fan¹, Lei Fu^{1,3,*}, Li Lin^{2,3,4,**}, Sheng Lai¹, Xin jie Huang¹, Yingqian Zhang⁵, Yunrong Luo¹, Xiulan Li¹, HaiZhou Zhang⁶

¹ School of Mechanical Engineering, Sichuan University of Science & Engineering

² Key Laboratory of Sichuan Colleges on Industry Process Equipment and Control Engineering

³ Key Laboratory of Material Corrosion and Protection of Sichuan Province

⁴ College of Materials and Chemistry and Chemical Engineering, Chengdu University of Technology

⁵ School of Civil Engineering, Sichuan University of Science & Engineering

⁶ Faculty of Intelligence Manufacturing, YiBin University

*E-mail: kunmingfulei@126.com; 1312019411@qq.com

Received: 16 May 2021 / Accepted: 8 July 2021 / Published: 10 August 2021

Aspergillus niger is a fungus that can promote the corrosion of aluminum alloys. In this paper, the corrosion behavior of 7075-T6 aluminum alloy in the presence of *Aspergillus niger* was investigated with the corrosion weight-loss method, electrochemical tests, scanning electron microscopy (SEM), and inductively coupled plasma optical emission spectrometry (ICP-OES). The results showed that *Aspergillus niger* greatly promoted the corrosion behavior of 7075-T6 aluminum alloy, and the corrosion rate was 6-12 times that of the sterile system. The electrochemical results showed that the corrosion process of the aluminum alloy was promoted by *Aspergillus niger*, and a large number of corrosion pits appeared on the surface with increasing exposure time. The research results confirmed that *Aspergillus niger* can significantly promote the corrosion of aluminum alloys.

Keywords: *Aspergillus niger*; Aluminum alloy; Microbiologically influenced corrosion; Electrochemical characteristics

1. INTRODUCTION

Aluminum alloys are widely used in the aerospace, automobile, shipbuilding, and chemical industries due to their great specific strength, thermal conductivity, corrosion resistance, and good processing properties. They have become the most widely used nonferrous metal material in industrial applications, and their usage is only inferior to that of steel materials[1-3]. Aluminum alloys can form an Al₂O₃ passivation film approximately 10~100 nm thick on their surfaces under natural conditions, which has a certain protective effect on the base material so that the aluminum alloy can exist stably

under natural conditions[4]. However, the passivation film is thin, porous, and discontinuous; it is easily broken and loses its protective effect when the aluminum alloy material is subjected to harsh environmental conditions during service, such as high-temperature, high-salt, and high-humidity conditions. The rupture of the oxide film could expose the matrix material to the atmosphere, thereby inducing corrosion failure[5]. Metal construction corrosion failure sometimes occurs. The processing technology and service environment of alloy materials are the key factors that determine their actual service life[6-9]. The corrosion morphology of aluminum alloys is mainly a localized corrosion morphology, and the common forms of corrosion are stress corrosion cracking, pit corrosion, crevice corrosion, galvanic corrosion, microbiological corrosion, etc.[10, 11].

The phenomenon that causes the corrosion of materials by the metabolic activities of various microorganisms is called microbiologically influenced corrosion (MIC)[12, 13]. There are two types of MIC: one is caused by metabolites, and the other is directly caused by electron transfer. Studies have shown that approximately 20% of the world's corrosion losses are caused by MIC[14, 15], and MIC is also an important cause of corrosion failure in structural materials. At present, most civil aircraft fuel tanks are still made of aluminum alloys, and aluminum alloys generally account for approximately 80% of consumption in civil aviation aircraft[16]. In 1958, microbial contamination blocked the fuel system of a bomber and caused it to crash in the United States. In 1996, many aircraft fuel tanks in China were corroded, and it was reported that this was one of the most serious aircraft fuel tank microbiological corrosion incidents in Chinese history[17]. As a result, an increasing number of researchers have begun to pay attention to MIC. Mold grows with hyphae, reproduces with spores, and has strong metabolic activity and vigorous vitality. It is one of the main microorganisms corrosive to metal materials and is widely present in various natural environments, such as the atmosphere, soil, and water. There are many kinds of molds can corrode and damage alloy materials, among them, the representative molds that are corrosive to aluminum alloy are *Aspergillus*, *Penicillium*, *Cladosporium*, and *Chaetomium*[18].

Aspergillus niger(*A. niger*) is an important mold that causes the microbial corrosion of aluminum alloys. According to the results of Wang[19], *A. niger* can significantly accelerate the uniform corrosion and local corrosion rates of 7075-T6 aluminum alloy in a high-salt environment. Compared with those of sterile systems, in the presence of *A. niger*, the uniform corrosion and local corrosion rates of the aluminum alloy increased by 3.7 times and 22.4 times, respectively. Dai[20] studied the corrosion behavior of 2024 aluminum alloy in NaCl systems, single *A. niger* systems, NaCl systems, and *A. niger* mixed systems, and the results showed that the presence of *A. niger* accelerated the corrosion of aluminum alloys. The corrosion rate of the aluminum alloy was more than 4 times that achieved in the NaCl system, and the oxalic acid produced by the metabolism of *A. niger* was the main cause of the corrosion of the 2024 aluminum alloy. Experiments have proven that the presence of *A. niger* could accelerate the corrosion of aluminum alloys to a certain extent. At present, it is believed that the mold corrosion mechanism of an aluminum alloy maybe includes the acid corrosion, concentration cell corrosion, and direct electron transfer mechanisms[21]. Studies by Miečinskis and Corvo[22, 23] showed that *A. niger* that attached to the surface of an aluminum alloy produced a large number of organic acids during its metabolic activities[24]. This reduced the pH of the surrounding environment and destroyed the passivation film of the aluminum alloy. The rupture of the passivation film promoted the corrosion of the aluminum alloy matrix and then constituted an acid corrosion process. *A. niger* is

an aerobic microorganism. In addition to the production of organic acids, it also consumes much oxygen during its metabolic activities, so the attached and unattached parts of *A. niger* on the aluminum alloy surface could form an oxygen concentration difference cell, which could accelerate the dissolution of the aluminum alloy anode area and lead to local corrosion[25, 26]. In the presence of mold, the cathode and anode reaction speeds of an aluminum alloy increased significantly[19], possibly due to the interaction between mold and the aluminum alloy accelerating the dissolution of the anode through direct electron transfer and causing local corrosion[23]. However, the direct electron transfer mechanism currently lacks direct evidence.

Aluminum alloys are currently one of the most commonly used alloy materials in engineering. Molds have simple growth conditions and rapid propagation speed, are widely present in nature and pose strong corrosion hazards to metal materials, especially aluminum alloys. Therefore, in this paper, 7075-T6 aluminum alloy was used as the base material to conduct a single directional culture of *A. niger* and to study the effect of *A. niger* on the corrosion of aluminum alloys. This paper used ICP-OES for the first time to detect the relationship between the contents of Al, Mg, Cu, and Fe in the soaking solution over time. The results showed that the precipitation of Al in the aluminum alloy in the *A. niger* system was significantly higher than that in the sterile systems. At the same time, the corrosion behavior of *A. niger* on aluminum alloys was studied by combining corrosion weight loss, SEM, and electrochemical testing methods, which has a certain theoretical basis and reference value for the systematic study of the corrosion of aluminum alloys by mold.

2. EXPERIMENTAL MATERIALS AND METHODS

2.1. Experimental materials

All specimens used in this work were 7075-T6 aluminum alloy, and the elemental compositions are shown in Table 1 (wt.%). The specimens used for electrochemical measurements were processed by wire cutting to obtain dimensions of 10 mm×10 mm×5 mm, and the working surface dimensions were 10 mm×10 mm. The back of the working surface was welded with copper wires, and all nonworking surfaces were sealed with epoxy resin. Specimens with dimensions of 50 mm×25 mm×3 mm were used for the weight loss test, and the corrosion morphology observation and composition analysis used a small coupon with processing dimensions of 16 mm×10 mm×3 mm. The work faces of all the specimens were abraded with 240-, 320-, 400-, 600- and 800-grit silicon carbide metallurgical papers in turn, degreased by acetone and anhydrous ethanol, dried with nitrogen, and placed in a desiccator for standby use. All specimens were put onto an ultraclean workbench and sanitized with an ultraviolet lamp for 30 minutes before use to ensure there was no contamination by other bacteria.

Table 1. Composition of 7075-T6 aluminum alloy (wt.%)

Si	Fe	Cu	Mn	Mg	Cr	Zn	Ti	Al
0.4	0.5	1.2~2.0	0.3	2.1~2.9	0.18~0.28	5.1~6.1	0.2	balance

2.2. Experimental medium

The *A. niger* used in this work came from the China Industrial Microbial Culture Collection and Management Center. For the cultivation of *A. niger*, potato dextrose liquid medium was selected. Potatoes were washed, peeled, and cut into small pieces. The potato pieces (200 g) and 1 L of deionized water were added to a pot, boiled for 30 min, and filtered with 4 layers of gauze. Glucose (20 g) was added to the filtrate, which was diluted to 1 L with deionized water, put in a high-pressure steam sterilization pot (LDZX-50KBS) at 115°C for 30 min, and then put in a refrigerator at 4°C for use after cooling. All aseptic operations were performed on a biologically clean bench (Suzhou Antai, BCM-1600A).

2.3. Weight loss measurements

The weight-loss method was used to calculate the corrosion rate of 7075-T6 aluminum alloy in *A. niger* solution and sterile solution (*A. niger* solution means potato dextrose liquid medium inoculated with *A. niger*, and sterile solution means potato dextrose liquid medium not inoculated with *A. niger*). Before the experiment, 24 large specimens and 16 small specimens were prepared (for morphological analysis). Among them, every 3 large specimens and 2 small specimens were divided into one group, for a total of 8 groups. Each large specimen was weighed before corrosion with an electronic balance, and all specimens were placed in a clean workbench and sanitized with a UV lamp for 30 minutes. Four groups were put into *A. niger* solutions, and the others were put into sterile solutions. All groups were placed in a constant-temperature shaking incubator at 30°C for 10 days, 15 days, 20 days, and 25 days. The exposed specimen surfaces were rinsed with a large amount of water, ultrasonically cleaned, cleaned in absolute ethanol and dried with N₂. The corrosion rate of the aluminum alloy was calculated by

$$V = \frac{W_0 - W_1}{St} \quad (1)$$

where V is the corrosion rate (g/cm²·h), W_0 is the mass of the specimen before corrosion (g), W_1 is the mass of the specimen processed to remove corrosion products after corrosion (g), S is the exposed specimen surface area (cm²), and t is the corrosion time (h).

2.4. Corrosion morphology and composition

After the weight loss measurements, each group took out a small specimen to remove the surface corrosion products and to dry with N₂. Scanning electron microscopy (SEM) was used to observe the corrosion morphology of aluminum alloys on different days in *A. niger* and sterile solutions. The other small specimens in each group that were dried directly with N₂ were characterized with X-ray energy spectrometry (EDS) to analyze the corrosion product components on their surfaces.

2.5 Determination of trace elements in the soaking solution

To explore the corrosion of aluminum alloys in the two solutions, inductively coupled plasma optical emission spectroscopy (ICP-OES) was used to measure the contents of the main alloy elements (aluminum, iron, zinc, and magnesium), the reasons for the changes in the contents of these four elements in the soaking solution were analyzed, and the corrosion mechanism of *A. niger* on the aluminum alloy was deduced. The preparation method of the test sample is as follows: 1 ml of the test solution was obtained, digested with a solution with a test solution:nitric acid:hydrochloric acid ratio=2:3:9, diluted to 100 ml, and stored at 4°C.

2.6. Electrochemical measurements

The electrochemical measurements used a standard three-electrode system: the working electrode was 7075-T6 aluminum alloy, the reference electrode was a saturated calomel electrode, and the auxiliary electrode was a platinum electrode. A electrochemical workstation (Chenhua GHI660E) was used to measure the open circuit potential (OCP) and to perform electrochemical impedance spectroscopy (EIS) for the working electrode in *A. niger* and sterile solutions. The OCP measurement time was 1800 s, the sampling interval was 0.1 s, the frequency range of the electrochemical impedance spectroscopy test was 10^{-2} Hz~ 10^5 Hz, and the excitation signal was a sine wave of 5 mV.

3. EXPERIMENTAL RESULTS AND DISCUSSION

3.1 Weight loss measurements

According to the weight loss corrosion equation (1), the average weight loss corrosion rates of the 7075-T6 aluminum alloy after 10, 15, 20, and 25 days in *A. niger* and sterile solutions were calculated, and the results are shown in Fig 1.

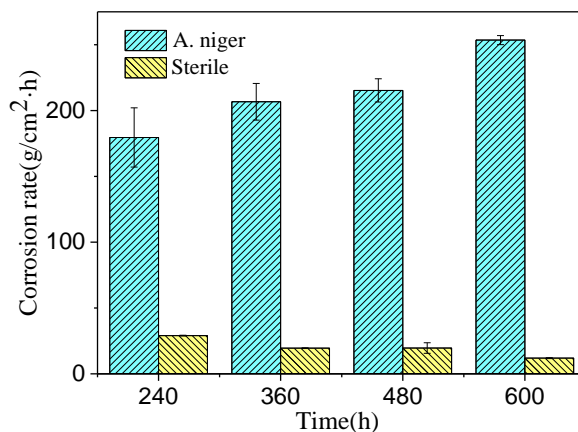


Figure 1. Corrosion rate of the 7075-T6 aluminum alloy after 10, 15, 20, and 25 days of exposure in different media at 30°C. The errors shown for each data point were the standard deviations obtained from three sets of measurements

Fig 1 shows that the corrosion rate of 7075-T6 aluminum alloy in the A. niger solution was significantly greater than that in the sterile solution, and the weight-loss corrosion rate in the A. niger solution was approximately 6-12 times that in the sterile solution. This result indicated that A. niger promoted the corrosion of the aluminum alloy. With the extension of the exposure time, the corrosion rate of the aluminum alloy gradually increased from 179 g/cm²·h on the 10th day to 253 g/cm²·h on the 25th day, which proved that the presence of A. niger could accelerate the corrosion of the aluminum alloy.

It was reported that the corrosion weight loss and corrosion time of metal materials conform to the following power function law[27-29]:

$$\Delta W = At^n \tag{2}$$

where ΔW is the corrosion weight loss (g/m²), t is the corrosion time (d), and A and n are constants. The value of n reflects the corrosion tendency of metal materials; $n < 1$ means that corrosion is weakened, and $n > 1$ means that corrosion is enhanced. The logarithm of both sides of equation (2) was taken to obtain the corresponding corrosion kinetic equation of the metal materials:

$$\log \Delta W = A + n \log t \tag{3}$$

Using t and ΔW to fit corrosion weight loss can yield the corrosion weight loss fitting curves of the aluminum alloy in the two systems (Fig 2). The corresponding fitting equations are shown in Table 2.

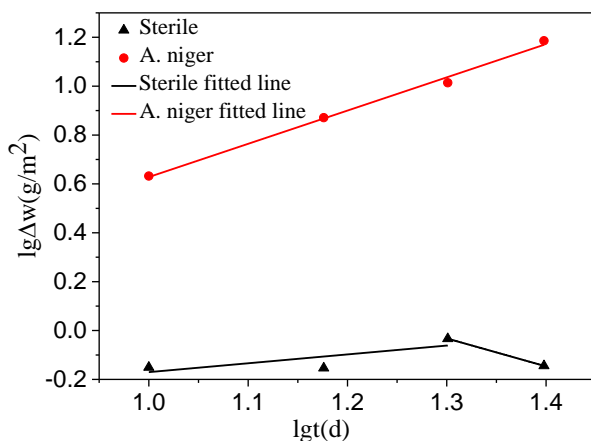


Figure 2. Corrosion weight loss fitting curves of 7075-T6 aluminum alloy in two solutions on different days

Table 2. Corrosion kinetic equation of 7075-T6 aluminum alloy in two solutions

system	stage	Fitted equation	the goodness of fit /R
A. niger	1	$\lg \Delta W = -0.73188 + 1.38 \lg t$	0.99744
	1	$\lg \Delta W = -0.53268 + 0.36248 \lg t$	0.79931
sterile	2	$\lg \Delta W = 1.45679 - 1.14539 \lg t$	1

Fig 2 shows that the corrosion weight loss in the sterile solution showed two stages, while the corrosion weight loss in the *A. niger* solution only had one stage. According to the corrosion kinetics fitting equation in Table 2, the value of n in the two stages in the sterile solution was less than 1, indicating that the corrosion tendency of aluminum alloy was weak in the sterile solution, which was due to the oxide film layer on the aluminum alloy surface having a certain protective effect on the substrate, making it less susceptible to corrosion. The value of n in the *A. niger* solutions was greater than 1, indicating that with the extension of the exposure time, the corrosion tendency of the aluminum alloy gradually increased, and the corrosion rate also increased, which was consistent with the corrosion rate in the *A. niger* solution shown in Fig 1. In general, when *A. niger* adhered to the aluminum alloy, it destroyed the oxide film and further corroded the aluminum alloys.

3.2 Scanning electron microscopy analysis

3.2.1 Corrosion morphology

Fig 3 shows a scanning electron microscopy image of 7075-T6 aluminum alloy exposed to *A. niger* and sterile solutions for different times after removing corrosion products, and the images are magnified 500 times.

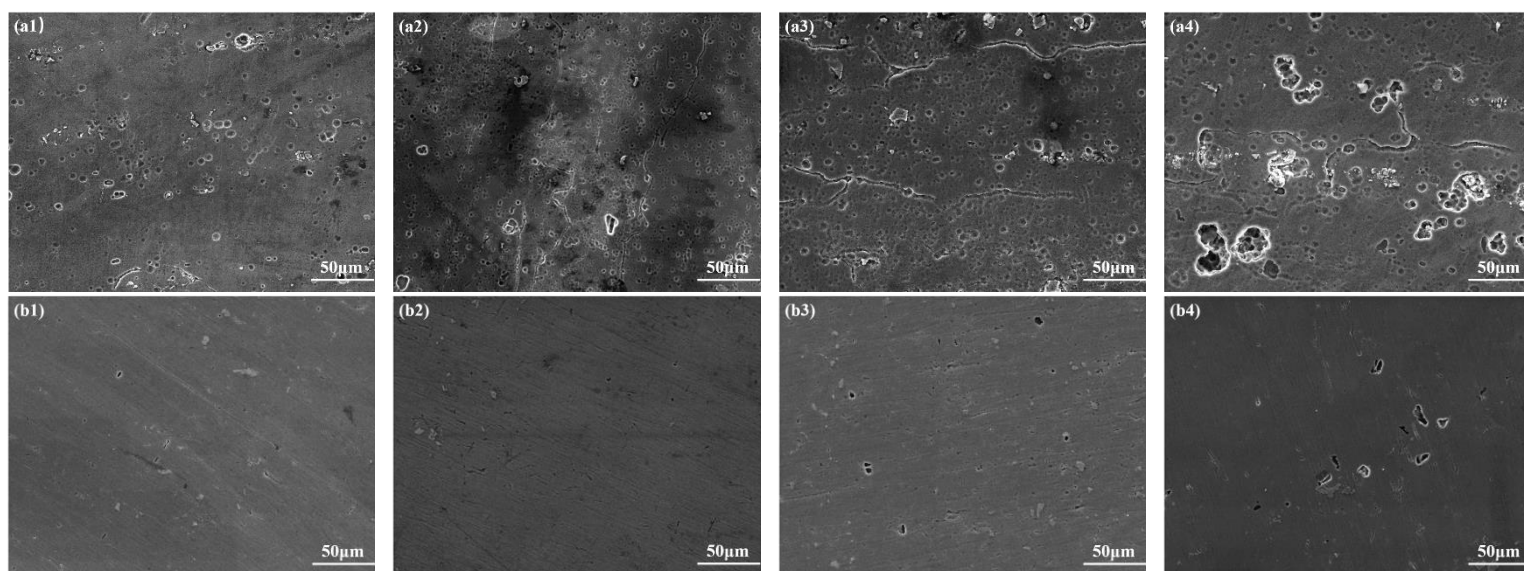


Figure 3. Scanning electron microscopy images of 7075-T6 aluminum alloy exposed to *A. niger* (a1, a2, a3, a4) and sterile (b1, b2, b3, b4) solutions at 30°C for 10, 15, 20, and 25 days after removing corrosion products

The SEM images show that in the sterile solutions (Fig 3 (b1-b4)), the surface of the aluminum alloy was smooth, and only some pitting corrosion appeared. This result indicates that the aluminum alloy was mainly uniformly corroded in the sterile system, and the corrosion tendency and corrosion rate

were both weak. After the aluminum alloy was exposed to the *A. niger* solution for 10 days (Fig 3 (a1)), many pits appeared, and this corrosion morphology was consistent with Wang's research results[19], indicating that the corrosion of the aluminum alloy by *A. niger* occurred mainly by local pitting. *A. niger* promoted the corrosion of the aluminum alloy, which was consistent with the corrosion weight loss results. With the extension of the exposure time (Fig 3 (a2-a3)), the number of pits on the surface of the aluminum alloy gradually increased. The amount of corrosion was too large, the pits interconnected to form larger corrosion pits on the 25th day (Fig 3 (a4)), and these pits reduced the mechanical properties and service life of the aluminum alloy to a certain extent.

According to the SEM images of 7075-T6 aluminum alloy in *A. niger* and sterile solutions (Fig 3), the corrosion forms and degrees of corrosion in the two systems were different. The cause of this phenomenon may be that the adhesion of *A. niger* to the surface of the aluminum alloy at the initial growth stage was random, which caused an uneven distribution of corrosion pits, and then, localized corrosion occurred. Some alloying elements in the aluminum alloy (such as Mg^{2+}) could promote the growth of *A. niger* to a certain extent[30]. As the exposure time increased, *A. niger* gradually accumulated and grew around these alloying elements. The metabolism of *A. niger* consumed electrons in the aluminum alloy, and Al lost electrons and became Al^{3+} , leading to the aluminum alloy matrix continuing to dissolve and eventually appearing as larger corrosion pits.

3.2.2 Energy spectrum analysis

Energy spectrum analysis was performed on the aluminum alloy specimen after 25 days of exposure in *A. niger* and sterile solutions before removing the corrosion products. The elemental distribution results are shown in Fig 4.

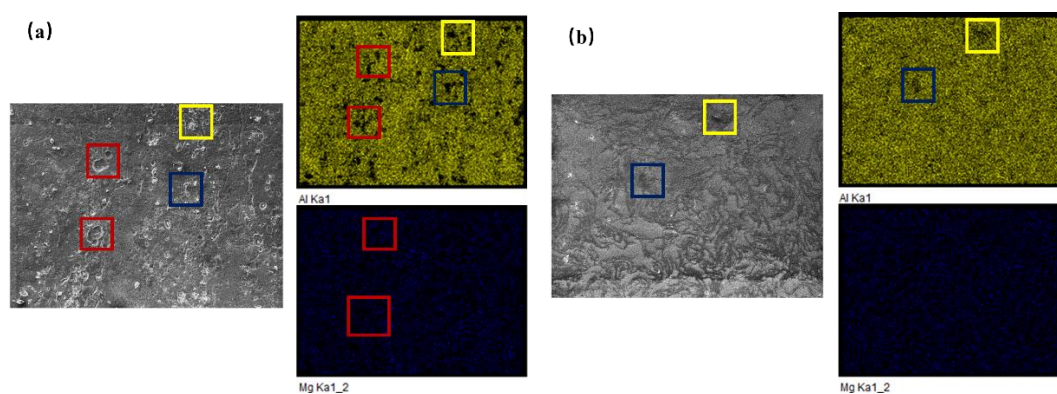


Figure 4. Elemental distribution (Al and Mg) on the surface of the aluminum alloy in the (a) *A. niger* and (b) sterile solutions

Based on the results of the EDS analysis, Fig 4(a) shows that in the *A. niger* solution, the aluminum content was significantly reduced at the corrosion pits, while there was little change in the content of magnesium. This result indicated that *A. niger* multiplied during magnesium enrichment and

caused severe corrosion of the aluminum alloy, but it did not cause severe corrosion of Mg, which was consistent with the research results of Li[30]. Fig 4(b) shows the distribution of elements on the surface in a sterile solution, and the degree of surface corrosion was relatively low. The content of aluminum was only slightly reduced in a few areas, and magnesium was evenly distributed, which was in sharp contrast with the observations in the *A. niger* solution.

3.3 Determination of trace elements in a corrosive solution

Inductively coupled plasma optical emission spectrometry was used to determine the contents of aluminum, iron, zinc, and magnesium in the corrosion solution and pure culture medium. The contents of the four elements in the pure medium are 0.04 mg/L Al, 0.29 mg/L Mg, 0.01 mg/L Zn, and 0.05 mg/L Fe; the corrosion solution results are shown in Fig 5.

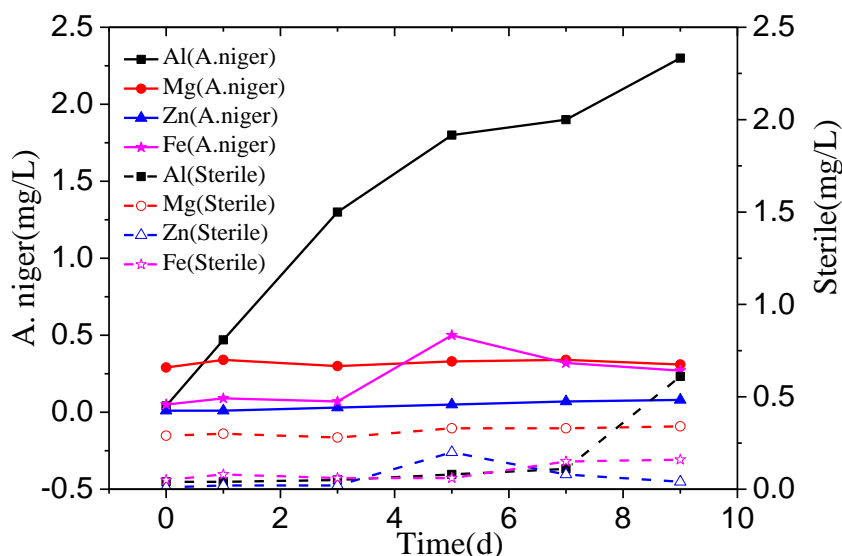


Figure 5. The contents of Al, Mg, Zn, and Fe in the *A. niger* solution and sterile solution over time

Fig 5 shows the content of each element in the *A. niger* and sterile solutions. In the early stage of exposure, the content of aluminum in the sterile solution changed little and was similar to that in the pure medium. The content of aluminum in the later stage of exposure showed a slight increase, which showed that the aluminum alloy was corroded to a certain extent in the sterile solution, but the corrosion degree was relatively low. In the *A. niger* solution, the content of aluminum continuously increased from 0.47 mg/L on the first day to 2.30 mg/L on the ninth day, indicating that *A. niger* accelerated the dissolution of aluminum in the aluminum alloy. This was due to *A. niger* adhering to the surface of the aluminum alloy and continuing to multiply, and aluminum precipitated from the alloy through its metabolism. The longer the *A. niger* was attached, the more aluminum that precipitated, and corrosion pits formed on the surface of the aluminum alloy. The changes in the contents of magnesium and zinc in the two systems were relatively small and were the same as those of magnesium and zinc in the pure

medium, indicating that *A. niger* did not accelerate the dissolution of magnesium and zinc in the alloy. The change in iron content may be because when *A. niger* corroded the aluminum alloy matrix, the corresponding alloy phase composition changed after aluminum was dissolved so that the iron element dissolved.

3.4 Electrochemical measurements

3.4.1 Open circuit potential

Electrochemical measurements were carried out in a modified electrochemical test reactor composed of a flat-bottomed four-necked flask. The OCP of the aluminum alloy in the *A. niger* and sterile solutions is shown in Fig 6.

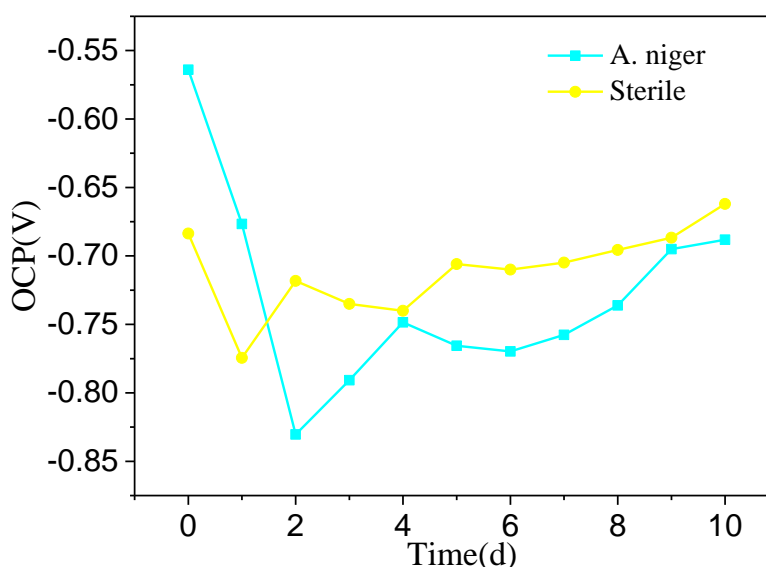


Figure 6. OCP of 7075-T6 aluminum alloy in two solutions

In the sterile solution, the OCP shifted positively during the first 2 days, slightly negatively shifted on days 3 and 4, gradually shifted positively and remained stable, showing a wave-like upward trend. In the *A. niger* solution, the OCP rapidly negatively shifted and changed significantly on the second day. This was due to the adhesion of *A. niger* on the surface in the initial stage of exposure and the formation of a discontinuous biofilm, which caused severe corrosion. From the 2nd to 9th days, *A. niger* continued to multiply, forming a dense and continuous biofilm on the surface, which played a certain protective effect on the specimen and reduced its corrosion tendency, so the OCP was positively shifted. At the same time, the dense biofilm also blocked the flow of oxygen[31]. Because *A. niger* is an aerobic microorganism, *A. niger* near the surface of the specimen died due to hypoxia, and the biofilm ruptured. The aluminum alloy matrix was exposed, and the corrosion tendency increased. After the inner biofilm ruptured and fell off, the outer *A. niger* continued to adhere. The dense biofilm reduced the

corrosion tendency, and the OCP shifted positively. This continued until the nutrients in the medium were exhausted and *A. niger* died.

The different changing trends of the OCP in the *A. niger* solution and the sterile solution indicated that *A. niger* affects the electrochemical corrosion of the aluminum alloy. The OCP in the *A. niger* solution was generally lower than that in the sterile solution, indicating that the presence of *A. niger* increased the corrosion tendency of the aluminum alloy and promoted corrosion.

3.4.2 EIS measurements

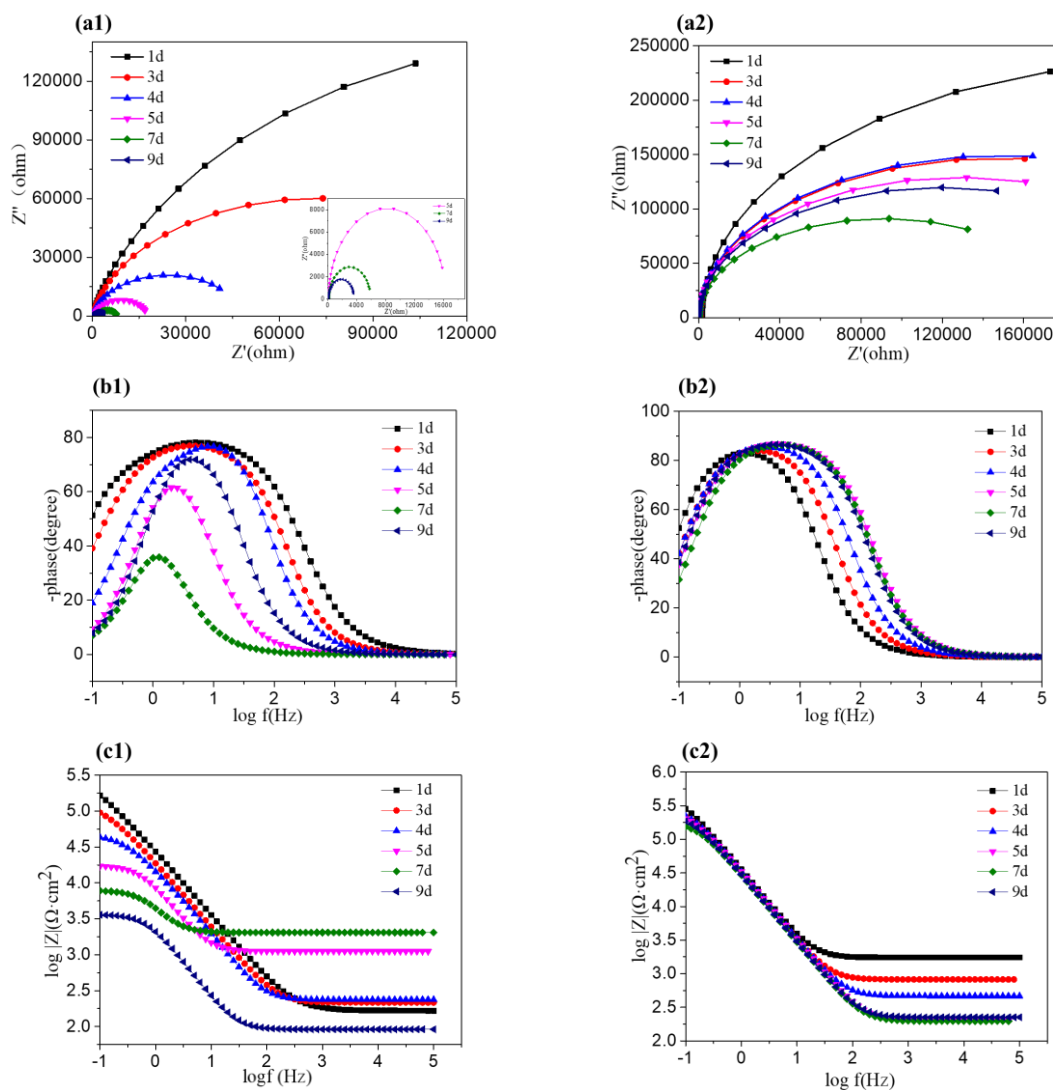


Figure 7. Nyquist and Bode plots of 7075-T6 aluminum alloy in two solutions: Nyquist plots in (a1) *A. niger* and (a2) sterile solutions and Bode plots in (b1) and (c1) *A. niger* and (b2) and (c2) sterile solutions

The EIS was performed on the aluminum alloy with different exposure times in the *A. niger* solution and the sterile solution at a stable open circuit potential, and the results are shown in Fig 7.

A remarkable difference observed from the Nyquist plots (Fig 7 (a1), (a2)) was that the diameters of the Nyquist loops obtained in the *A. niger* solution were smaller than those obtained in the sterile solution. This result demonstrates that the corrosion process was promoted by *A. niger*, which is consistent with the results of the corrosion rate test (Fig 1). For specimens in *A. niger* (Fig 7 (a1)), the diameters of the Nyquist loops decreased with time, suggesting that *A. niger* attached to the specimen surface and produced a large amount of organic acids, such as oxalic acid[20], which lowered the pH of the *A. niger* solution[32] due to its metabolic activity, which destroyed the passivation film and accelerated the corrosion tendency. The impedance modulus of the aluminum alloy dropped by approximately 1.5 times (Fig 7 (c1)). Throughout the test cycle, the diameter of the Nyquist loops obtained in the *A. niger* solution (Fig 7 (a1)) and the impedance modulus (Fig 7(c1)) constantly decreased, which proved that *A. niger* continued to corrode the aluminum alloy. In combination with the change in corrosion rate (Fig 1), the total corrosion degree gradually increased. For sterile solutions (Fig 7 (b2), (c2)), the impedance modulus had a small change and was stable within a certain range, suggesting that the aluminum alloy did not corrode during the test period.

During the microbial corrosion of metal materials, bacterial activity, biofilm structures, and metabolites can affect the electrochemical reaction in the corrosion process[33]. In the *A. niger* solution, the phase angle peak of the Bode plot (Fig 7(b1)) gradually shifted to a lower frequency from the 1st to 7th days, indicating that the biofilm continuously formed on the aluminum alloy surface. On the 7th to 9th days, the phase angle shifted to a higher frequency, suggesting that the biofilm began to rupture[34], which may be caused by the exhaustion of nutrients in the medium and the death of *A. niger*.

The impedance spectra in Fig 7 were curve-fitted with Zview2 software (Fig 8). R_s is the solution resistance, Q_f and R_f are the capacitance and resistance of the biofilm, respectively, Q_{dl} and C_{dl} are the solution double-electron layer capacitance, and R_{ct} is the charge transfer resistance. The equivalent circuit of the sterile system was expressed as R(CR), and the equivalent circuit of the *A. niger* system was expressed as R(Q(R(QR))) in the early stage and R(CR) in the later stage. This was because the biofilm ruptured in the later stage, and R_f decreased drastically and accelerated the corrosion of the aluminum alloy. The corresponding fitting data is shown in Table 3.

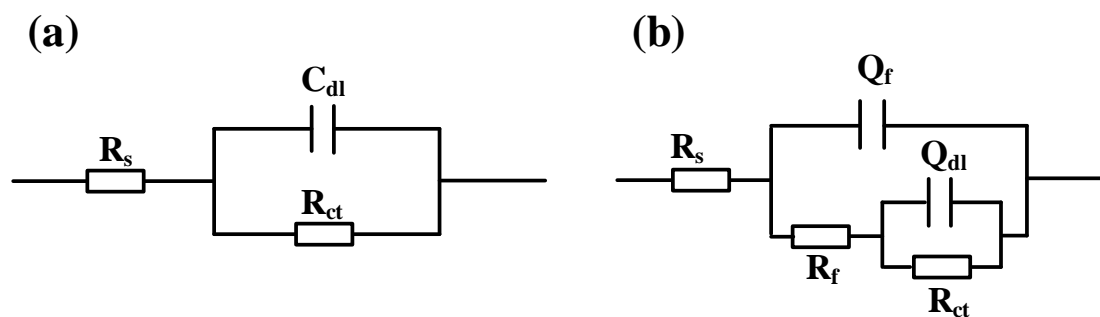


Figure 8. Equivalent circuit in two solutions

Table 3. Impedance fitting results of the aluminum alloy in two solutions

Systems	Time (d)	R_s ($\Omega \text{ cm}^2$)	Q_{dl}/C_{dl} ($\Omega^{-1} \text{ s}^n \text{ cm}^{-2}$)	n_1	R_f ($\Omega \text{ cm}^2$)	Q_f ($\Omega^{-1} \text{ s}^n \text{ cm}^{-2}$)	n_2	R_{ct} ($\Omega \text{ cm}^2$)
A. niger	1	165.9	5.623×10^{-6}	0.9021	2.23×10^5	6.713×10^{-6}	0.9995	1.09×10^5
	3	216.1	5.397×10^{-6}	1	1.478×10^5	5.204×10^{-6}	0.7537	1.459×10^5
	4	237.3	8.805×10^{-6}	1	1.514×10^4	8.035×10^{-6}	0.8228	3.226×10^4
	5	1112	1.747×10^{-5}	-	-	-	-	1.628×10^4
	7	2038	4.512×10^{-5}	-	-	-	-	5794
	9	91.26	6.384×10^{-5}	-	-	-	-	3541
Sterile	1	1745	4.471×10^{-6}	-	-	-	-	4.701×10^5
	3	821.1	4.961×10^{-6}	-	-	-	-	2.934×10^5
	4	466.3	4.828×10^{-6}	-	-	-	-	2.986×10^5
	5	548.7	5.141×10^{-6}	-	-	-	-	2.649×10^5
	7	250.8	5.484×10^{-6}	-	-	-	-	1.829×10^5
	9	225.2	5.296×10^{-6}	-	-	-	-	2.394×10^5

Table 3 shows that the solution resistance R_s and the charge transfer resistance R_{ct} in the sterile solution remained at the same order of magnitude during the test period, which proved that the aluminum alloy was not corroded or had a low degree of corrosion in the sterile solution. This was consistent with the Bode plot change (Fig 7 (b2), (c2)). In the A. niger solution, R_f and R_{ct} decreased significantly on the 4th day, and the corrosion rate increased. The rupture of the biofilm in the later stage reduced R_f to almost zero, and the equivalent corrosion circuit became R(CR). With the extension of the exposure time, the sum of the resistances in the solution decreased, and the corrosion rate of the aluminum alloy in the A. niger solution increased constantly.

3.5 Corrosion mechanism discussion

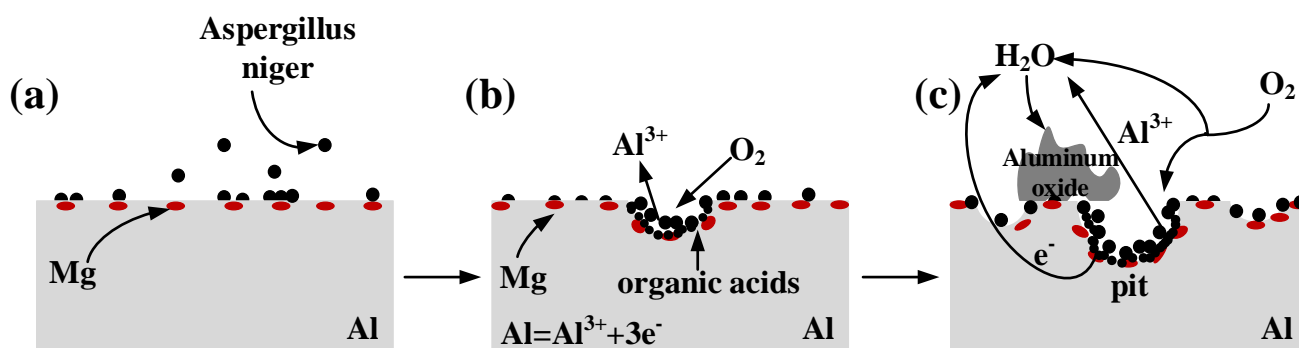


Figure 9. Schematic diagram of the local corrosion on the aluminum alloy by A. niger: (a) A. niger adhered to the surface, (b) A. niger producing organic acids and corroding the base material, and (c) the expansion of pits and corrosion product accumulation

The present results confirmed that A. niger increased the corrosion tendency, increased the corrosion rate, and promoted the corrosion of the aluminum alloy. Based on the results of the weight

loss, corrosion morphology, ICP-OES, and electrochemical analyses, the corrosion mechanism of 7075-T6 aluminum alloy in the *A. niger* solution could be divided into three stages, as shown in Fig 9.

In the early stage (Fig 9(a)), *A. niger* preferentially grew on the Al-Mg intercrystalline area[30] and gradually formed a biofilm on the surface of the aluminum alloy. In the middle of the expose (Fig 9(b)), the metabolic activity of *A. niger* on the surface of the aluminum alloy produced amylase, acid protease, cellulase, pectinase, glucose oxidase, citric acid, gluconic acid and other organic acids, such as oxalic acid. Oxalic acid is the main component of the metabolites of *A. niger* and is the cause of the severe corrosion of the aluminum alloy[35]. At the same time, the metabolic activity of *A. niger* also consumed O₂ and formed a local hypoxic environment, which destroyed the passivation film and caused local corrosion, releasing Al³⁺ [21]. The lack of O₂ causes *A. niger* on the surface of the aluminum alloy to gradually lose its activity. Then, the outer layer of *A. niger* was attached again, and the corrosion process continued in this cycle. Finally, (Fig 9(c)), the released Al³⁺ reacted with the anions (OH⁻ and O²⁻) in the solution to form aluminum oxide precipitates (Al(OH)₃, Al₂O₃, etc.)[31]. As the corrosion process continued, corrosion products accumulated on the surface, which protected the aluminum alloy, thereby decreasing the local corrosion rate. The corrosion mechanism for *A. niger* can be expressed as follows:



4. CONCLUSION

The experimental results showed that *A. niger* can promote the corrosion of aluminum alloys. EIS confirmed that aluminum alloys have a greater tendency to corrode in *A. niger* solutions. The SEM and corrosion weight loss results also proved that the corrosion of the aluminum alloy by *A. niger* changes with time. During the test period, the corrosion rate in the *A. niger* solution was 6-12 times that in the sterile solution. With the extension of the time, the pitting corrosion degree in the *A. niger* system gradually increased, and the area of corrosion pits continued to increase. The ICP-OES results proved that the presence of *A. niger* can lead aluminum to dissolve to Al³⁺ and form corrosion pits on the surface, which aggravates the corrosion of the aluminum alloy.

ACKNOWLEDGMENTS

This work was financially supported by National Nature Science Foundation of China (No.51701133), the Opening Project of Key Laboratory of Material Corrosion and Protection of Sichuan Province (No. 2020CL18), the undergraduate innovation and business startups training program of SUSE (No. CX2020012), the Opening Foundation of Sichuan Province Engineering Center for Powder Metallurgy(SC-FMYJ2019-07), the Project of Key Lab in Sichuan Colleges on Industry Process Equipment and Control Engineering (GK201808, GK201816, GK202004, GK202108) and Talent Introduction Project of Sichuan University of Science and Engineering(2020RC19).

References

1. R. Arrabal, B. Mingo, A. Pardo, M. Mohedano, E. Matykina and I. Rodriguez, *Corros. Sci.*, 73 (2013) 342.
2. G. Gaustad, E. Olivetti and R. Kirchain, *Resour. Conserv. Recycl.*, 58 (2012) 79.
3. M. C. Reboul and B. Baroux, *Mater. Corros.*, 62 (2015) 215.
4. M. Teng, Z. Y. Wang and W. Han, *Corrosion Science and Protection Technology*, 03 (2004) 155.
5. X. Wei and S. Wang, *New Technology & New Process*, 06 (2019) 9.
6. P. Dong, Z. Liu, X. Zhai, Z. Yan, W. Wang and P. K. Liaw, *Int. J. Fatigue*, 124 (2019) 15.
7. J. M. Bastidas, A. Forn, C. L. Torres, M. T. Baile and J. L. Polo, *Mater. Corros.*, 52 (2001) 691.
8. C. N. Panagopoulos, E. P. Georgiou and K. I. Giannakopoulos, *Mater. Corros.*, 60 (2015) 415.
9. D. Prabhu and P. Rao, *Arabian J. Chem.*, 10 (2017) S2234.
10. A. Venugopal, R. Panda, S. Manwatkar, K. Sreekumar, L. Ramakrishna and G. Sundararajan, *Trans. Nonferrous Met. Soc. China*, 22 (2012) 700.
11. A. Chateaufneuf, F. Cochetoux, F. Deffarges and F. Sourget, *Proc. Inst. Mech. Eng., Part O: J. Risk Reliab.*, 225 (2011) 293.
12. M. Lv and D. Min, *Rev. Environ. Sci. Biotechnol.*, 17(2018) 1.
13. K. M. E. Emde, D. W. Smith and R. Facey, *Pergamon*, 26 (1992) 169.
14. C. M. Xu, Y. H. Zhang, G. X. Cheng and W. S. Zhu, *Mater. Sci. Eng., A*, A443 (2007) 235.
15. H. Castaneda and X. D. Benetton, *Corros. Sci.*, 50 (2008) 1169.
16. T. Dursun and C. Soutis, *Mater. Des.*, 56 (2014) 862.
17. X. D. Yin and B. Wan, *Corrosion & Protection*, 040 (2019) 366.
18. J. T. Zhang and Y. L. Wu, *Equipment Environmental Engineering*, 06 (2007) 70.
19. J. L. Wang, F. P. Xiong, H. W. Liu, T. S. Zhang, Y. Y. Li, C. J. Li, W. Xia, H. T. Wang and H. F. Liu, *Bioelectrochem. Bioenerg.*, 129 (2019) 10.
20. X. Y. Dai, H. Wang, L. K. W. Ju, G. Cheng, H. B. Cong and B. Z. Newby, *Int. Biodeterior. Biodegrad.*, 115 (2016) 1.
21. U. Jirón-Lazos, F. Corvo, L. De, E. M. García-Ochoa, D. M. Bastidas and J. M. Bastidas, *Int. Biodeterior. Biodegrad.*, 133 (2018) 17.
22. P. Miečinskis, K. Leinartas, V. Uksienė-Eimutis and Juzeliūnas, *J. Solid State Electrochem.*, 11 (2007) 909.
23. F. Corvo, S. D. L. Rosa, D. M. Bastidas, U. Jirón-Lazos and J. M. Bastidas, Aluminum and anodized aluminum biocorrosion caused by *Aspergillus niger*, proceedings of the Latincorr, Latincorr2016, Mexico, 2016.
24. E. Juzeliūnas, R. Ramanauskas, A. Lugauskas, M. Samuleviien and K. Leinartas, *Electrochem. Commun.*, 7 (2005) 305.
25. L. L. Machuca, S. I. Bailey, R. Gubner, E. L. J. Watkin, M. P. Ginige, A. H. Kaksonen and K. Heidersbach, *Corros. Sci.*, 67 (2013) 242.
26. A. Heyer, F. D. Souza, C. F. L. Morales, G. Ferrari, J. M. C. Mol and J. H. W. de Wit, *Ocean Eng.*, 70 (2013) 188.
27. Y. T. Ma, Y. Li and F. H. Wang, *Corros. Sci.*, 52 (2010) 1796.
28. S. X. Wang, N. Du, D. X. Liu, J. H. Xiao and D. P. Deng, *Journal of Chinese Society for Corrosion and Protection*, 39 (2019) 20.
29. X. G. Li, Initial behavior and mechanism of atmospheric corrosion for metal, Science Press, (2009) Beijing, China.
30. C. J. Li, Effect of *Aspergillus niger* on corrosion behavior of 7075 aluminum alloy and its protection methods, (2019) Wuhan, Huazhong University of Science & Technology.
31. Q. Qu, S. Li, L. Li, L. Zuo, X. Ran, Y. Qu and B. Zhu, *Corros. Sci.*, 118 (2017) 12.
32. J. L. Wang, C. L. Li, X. X. Zhang, M. Asif, T. S. Zhang, B. S. Hou, Y. Y. Li, W. Xia, H. T. Wang and H. F. Liu, *J. Electrochem. Soc.*, 166 (2019) G39.

33. M. Lv, M. Du, X. Li, Y. Yue and X. Chen, *J. Mater. Res. Technol.*, 8 (2019) 4066.

34. A. P. Yadav, A. Nishikata and T. Tsuru, *Corros. Sci.*, 46 (2004) 169.

35. T. S. Zhang, J. L. Wang, G. A. Zhang and H. F. Liu, *Corros. Sci.*, 176(2020) 108930.

© 2021 The Authors. Published by ESG (www.electrochemsci.org). This article is an open access article distributed under the terms and conditions of the Creative Commons Attribution license (<http://creativecommons.org/licenses/by/4.0/>).